Convergent evolution of tree hydraulic traits in Amazonian habitats: implications for community assemblage and vulnerability to drought

Clarissa G. Fontes[1,9] (iD), Paul V. A. Fine[1] (iD), Florian Wittmann[2,3] (iD), Paulo R. L. Bittencourt[4] (iD), Maria Teresa Fernandez Piedade[5] (iD), Niro Higuchi[6] (iD), Jeffrey Q. Chambers[7,8] (iD) and Todd E. Dawson[1] (iD)

[1]Department of Integrative Biology, University of California, Berkeley, Berkeley, CA 94720, USA; [2]Department of Wetland Ecology, Institute of Geography and Geoecology, Karlsruhe Institute of Technology – KIT, Josefstr.1, Rastatt D-76437, Germany; [3]Biogeochemistry, Max Planck Institute for Chemistry, Hahn-Meitner Weg 1, Mainz 55128, Germany; [4]College of Life and Environmental Sciences, University of Exeter, Exeter, EX4 4RJ, UK; [5]Coordenação de Dinâmica Ambiental, Instituto Nacional de Pesquisas da Amazônia – INPA, Av. André Araújo, Petrópolis, Manaus, AM 2936, 69067-375, Brazil; [6]Ciências de Florestas Tropicais, Instituto Nacional de Pesquisas da Amazônia (INPA), Manaus, AM 69067-375, Brazil; [7]Climate Science Department, Climate and Ecosystem Sciences Division, Lawrence Berkeley National Laboratory, One Cyclotron Road, Building 74, Berkeley, CA 94720, USA; [8]Department of Geography, University of California Berkeley, 507 McCone Hall #4740, Berkeley, CA 94720, USA; [9]Department of Ecology, Evolution and Behavior, University of Minnesota, 1479 Gortner Avenue, Saint Paul, MN 55108, USA

Summary

• Amazonian droughts are increasing in frequency and severity. However, little is known about how this may influence species-specific vulnerability to drought across different ecosystem types.

• We measured 16 functional traits for 16 congeneric species from six families and eight genera restricted to floodplain, swamp, white-sand or plateau forests of Central Amazonia. We investigated whether habitat distributions can be explained by species hydraulic strategies, and if habitat specialists differ in their vulnerability to embolism that would make water transport difficult during drought periods.

• We found strong functional differences among species. Nonflooded species had higher wood specific gravity and lower stomatal density, whereas flooded species had wider vessels, and higher leaf and xylem hydraulic conductivity. The P_{50} values (water potential at 50% loss of hydraulic conductivity) of nonflooded species were significantly more negative than flooded species. However, we found no differences in hydraulic safety margin among species, suggesting that all trees may be equally likely to experience hydraulic failure during severe droughts.

• Water availability imposes a strong selection leading to differentiation of plant hydraulic strategies among species and may underlie patterns of adaptive radiation in many tropical tree genera. Our results have important implications for modeling species distribution and resilience under future climate scenarios.

Introduction

The Amazon Basin occupies an area of *c.* 7 million km^2 and is the largest and most biodiverse tropical rainforest in the world (Ribeiro *et al.*, 1999). The main vegetation types found in the Amazon Basin are mature *terra-firme* forests (plateau/upland, valley and slope forests; approx. 63% of Amazon Basin), woodland savanna (*c.* 22%), floodplain/inundated forests (*c.* 10%), secondary forest and white-sand areas (*c.* 5%; Saatchi *et al.*, 2007; Adeney *et al.*, 2016; Wittmann & Junk, 2016). These distinct habitats differ mainly in soil type, plant water availability, and topography. This great environmental heterogeneity has been proposed as one of the main explanations for the high diversity of

tree species in Amazonian tropical ecosystems (Connell, 1978; Smith *et al.*, 1997; ter Steege *et al.*, 2000). Environmental heterogeneity can promote ecologically-mediated speciation and habitat specialization, and thus increase beta-diversity among areas (Tuomisto *et al.*, 2003; Fine & Kembel, 2011; Wittmann *et al.*, 2013; Fine, 2015; Leibold & Chase, 2017). Indeed, several studies have reported high tree species turnover in the different Amazonian habitats (e.g. ter Steege *et al.*, 2000; Valencia *et al.*, 2004; Stropp *et al.*, 2011; Schietti *et al.*, 2014; Assis *et al.*, 2015). Moreover, a large number of studies have tested for edaphic and topographic habitat specialization among tropical trees (e.g. Phillips *et al.*, 2003; Fine & Kembel, 2011; Damasco *et al.*, 2013; Toledo *et al.*, 2017). However, despite the strong differences in plant

water availability among these diverse Amazonian habitats, relatively little attention has been paid to how water availability can be linked to tree species distribution in Amazonian forests (but see Schietti *et al.*, 2014; Oliveira *et al.*, 2019), which is particularly important to understand in face of the rapid climatic and land-use change currently taking place in the Amazon Basin.

Extreme drought events are becoming more frequent and intense in the Amazon (Marengo *et al.*, 2011; Fu *et al.*, 2013; Stocker *et al.*, 2013), and many studies have linked warmer and drier conditions to increased levels of tree physiological stress in tropical areas (Doughty & Goulden, 2008; Bonal *et al.*, 2016; Tng *et al.*, 2018; Fontes *et al.*, 2018b). Overall precipitation also is predicted to decrease across the Amazonian region (Stocker *et al.*, 2013; Marengo *et al.*, 2018), and this would have profound effects on the water availability for trees. Contrasting environments with distinct water availabilities may select on species hydraulic strategies, resulting in water-driven distributions of plant communities (Engelbrecht *et al.*, 2007; Blackman *et al.*, 2014; Cosme *et al.*, 2017). Furthermore, some studies have suggested that species from Amazonian floodplain forests inundated by black-water rivers may be more vulnerable to drought than plateau species (Parolin & Wittmann, 2010; Zuleta *et al.*, 2017; Oliveira *et al.*, 2019). However, the physiological mechanism for this assertion has not been fully explored and the drought vulnerability of species from different Amazonian habitats has yet to be tested. Thus, to understand the effect of future climate in the world's largest tropical forest, it is of paramount importance to know how water limitation may shape species distributions in the contrasting Amazonian ecosystems, and how these communities differ in their vulnerability to predicted water deficit.

Hydraulic traits such as P_{50} (the water potential at which plants lose 50% of their hydraulic conductivity) and stem safety margin (SM = minimum water potential measured in the field – P_{50}) are used widely to assess vulnerability and response of plants to drought (Choat *et al.*, 2012; Skelton *et al.*, 2015; Fontes *et al.*, 2018b). P_{50} is a measure of how vulnerable xylem vessels are to embolism; embolism resistance has been shown to have a positive relationship with the intensity of drought stress experienced by plants across many terrestrial ecosystems (Choat *et al.*, 2012; Blackman *et al.*, 2014; Oliveira *et al.*, 2019). By contrast, SM indicates how close plants operate to the point of xylem disfunction (Meinzer *et al.*, 2009; Klein *et al.*, 2014; Bucci *et al.*, 2016). At the global scale, SM has been shown to be independent of water availability and plant species from contrasting ecosystems (e.g. desert vs tropical forest) may have similar SM values (Choat *et al.*, 2012), which is consistent with the idea that plants from a broad range of environments converge in operating close to their hydraulic limit as a way of maximizing carbon uptake. However, it is still unclear if these patterns also are found at local scales, and, to our knowledge, this has never been tested within different tropical ecosystems. Furthermore, hydraulic trait variation across tropical rainforest tree taxa remains poorly resolved. Therefore, the Amazon is still under-represented in global hydraulic trait datasets, likely because of the high species diversity, the

inaccessibility of remote sites, and the time-consuming quantification of plant hydraulic traits.

We measured 16 leaf, wood and hydraulic traits of 16 tree species from eight genera exhibiting contrasting distributions across four main Amazonian habitats, making this the most comprehensive study to date on plant hydraulic strategies in the Amazon. All habitats are under the same climatic regime and any differences in water availability are likely due to soil type, topography and/or ground water amounts. We sampled two habitats (flooded habitats) where water is constantly available throughout the year (a periodically flooded black-water floodplain forest along a low-order river and a permanently saturated swamp forest in the catchment area of a high-order creek) and another two habitats (nonflooded habitats) where water is markedly limited during the dry season (white-sand and plateau forests) to test the following hypotheses: (H1) flooded habitat species (floodplain and swamp forests) will be more vulnerable to xylem embolism than species from nonflooded (drier) habitats (plateau and white-sand forest) in the Amazon; (H2) if the same pattern of hydraulic safety margin (SM) reported at global scales – convergence to low SM – is observed at local scales, we hypothesize that independent of site water availability, Amazonian trees will operate with similar hydraulic safety margin, in a way of maximize carbon uptake; (H3) congeneric species from contrasting environments in the Amazon will differ in their leaf, wood and hydraulic traits, consistent with the hypothesis that these trait differences have evolved repeatedly and independently in the distinct close phylogenetic lineages probably due to selective environmental pressure (habitat-mediated ecological speciation).

Materials and Methods

Study site

Our two study sites are located at Reserva Biológica do Cuieiras/ Estação Experimental de Silvicultura Tropical, also known as ZF-2 (lat. 2°36′33″S, long. 60°12′33″W), and at the Uatumã Sustainable Development Reserve (USDR), where the Amazon Tall Tower Observatory, ATTO, is situated (lat. 2°08′38″S, long. 58°59′59″W). The ZF-2 and ATTO are located, respectively, *c.* 90 km NW and *c.* 150 km NE of the city of Manaus-AM, Brazil. The ZF-2 site is covered by 31 000 ha of dense humid *terra-firme* forest, with a mean canopy height of *c.* 28 m (Roberts *et al.*, 1996; Kunert *et al.*, 2017). The mean annual precipitation between 2002 and 2016 was 2140 mm, and the mean annual temperature was 28°C (Fontes *et al.*, 2018b). The USDR (ATTO site) consists of different forested ecosystems, which include dense, nonflooded upland forests (*terra-firme*), white-sand forests and seasonally flooded black-water floodplain forest along the Uatumã River and several smaller tributaries. The annual average precipitation and temperature between 2012 and 2014 were 2376 mm and 28°C, respectively. The dry season for both areas is from July to September when precipitation generally is < 100 mm. For a detailed description of the ZF-2 site, refer to (Fontes *et al.*, 2018a,b) and for ATTO see (Andreae *et al.*, 2015; Targhetta *et al.*, 2015).

Environmental variables

We used soil texture (percentage of clay and sand fraction), and water table depth (minimum and maximum) to characterize soil and water availability in each of the plots where the trees were collected. Water table depth for the ZF-2 site from 2014 to 2016 was provided by the LBA Hydrology group. The raw data are available upon request from the LBA Hydrology Group from: http://lba2.inpa.gov.br/index.php/dados-hidrologicos.html. The topsoil texture data for ZF-2 were obtained from (Ferraz *et al.*, 1998), where they analyzed soil texture in the first 30 cm of the soil. For the ATTO site, data of water table depth and topsoil texture were extracted from previous studies (Andreae *et al.*, 2015; Targhetta *et al.*, 2015). Soil texture was obtained from the first 20cm of the soil and water table depth was collected between 2009 and 2011 (Targhetta *et al.*, 2015). A detailed characterization of the water availability and soil texture of each location/habitat type that we sampled can be found in the section below.

Habitat types

We sampled from four contrasting environments: black-water seasonal floodplain forest (BFF; also known as 'igapó'), swamp forests (S; also known as 'baixios' or valley forests), plateau (P; also known as *terra-firme*) and white-sand forest (WS; also known as *campinarana*; Fig. 1). These four habitats cover the main gradients of soil texture, fertility, water availability (water table depth), and forest structure found in the central Amazon Basin (Fortunel *et al.*, 2014). Furthermore, the habitats can be divided into two main water regimes (flooded and nonflooded) and two soil types (clay and sandy) as shown in Table 1. Therefore, for each water regime type, we sampled one habitat that had clay soil and one that had predominantly sandy soils.

The soil texture in the BFF of the Uatumã river is predominantly clay but nutrient-poor, with pH values (H_2O) of 4.05 ± 0.2 (Supporting Information Table S1; Targhetta *et al.*, 2015). These forests have comparatively low tree species richness with 26–49 species ha^{-1} (diameter at breast height (DBH) ≥ 10 cm) and the mean flood height is 2.77 ± 0.9 m for ≤ 230 d yr^{-1} (Table S1; Targhetta *et al.*, 2015). Swamp habitats are the lower riparian areas with soil sand content varying from 77% to 83% (Ferraz *et al.*, 1998). The swamp forests feature almost no topographic variation, with the water table close to the surface (≤ 1 m deep), and soils permanently or seasonally waterlogged during the rainy season (Tomasella *et al.*, 2008). The plateau forests are generally flat or have gentle slopes (< 7%) with absolute elevation varying between 90 m and 120 m asl in our study area. The soils have a high fraction of clay content (80–90-%), and the water table can reach *c.* 20 m deep (Tomasella *et al.*, 2008). Finally, the white-sand forests of ATTO are characterized by nutrient-poor soils with high acidity (Targhetta *et al.*, 2015). With 93.3 ± 1.5%, the sand fraction in the soil is high, and water table depth can reach 4 m deep. Because of the lower stature of trees, white-sand forests have a high incidence of solar radiation and leaf temperature can be 3–5°C higher than in plateau forests
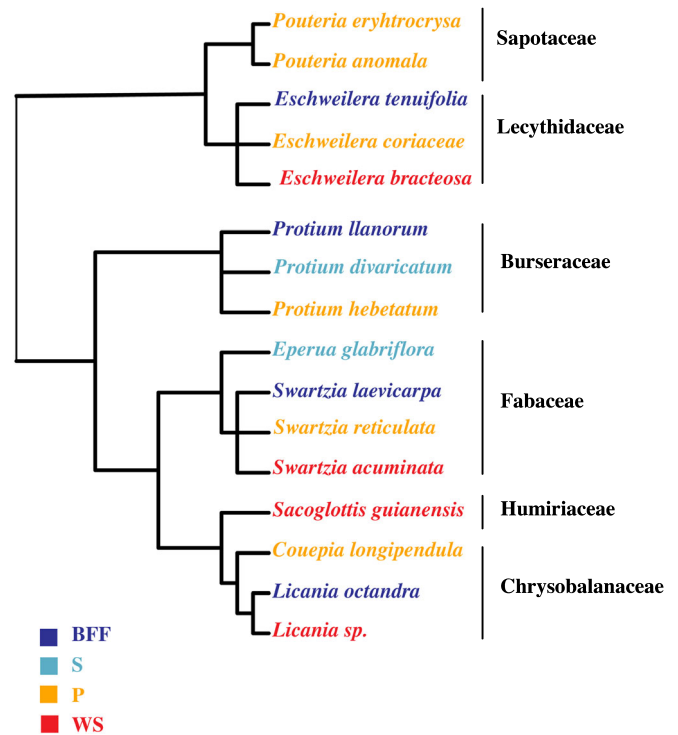
Fig. 1 The evolutionary relationship of 16 tropical tree species selected for this study. The cladogram is based on the maximum resolved angiosperm phylogeny (APG III R20120829). Colors indicate the four different habitats where the species are mainly found: BFF, black-water seasonal floodplain forest; S, swamp forests; P, plateau; WS, white-sand forest.

Table 1 Summary table of the location, water regime and soil texture of the four habitats analyzed in our study.

Habitat	Abbreviation	Location	Water regime	Soil texture
Black-water seasonal floodplain forest (also known as 'igapó')	BFF	ATTO	Flooded	Clay
Swamp forests (aka 'baixios' or valley forests)	S	ZF-2	Flooded	Sand
Plateau (aka 'terra-firme')	P	ZF-2	Nonflooded	Clay
White-sand forest (aka 'campinarana')	WS	ATTO	Nonflooded	Sand

(Medina *et al.*, 1978; Rinne *et al.*, 2002). This habitat can become very dry and hot during the dry season. In summary, the four habitats differ greatly in their soil texture and water regime (Fig. 2), indicating a strong environmental difference among these habitats. (For more information about the differences in forest structure among the four environments refer to Table S1.)

Species selection

We selected 16 species from the database of permanent plots (DBH ≥ 10 cm) located at ATTO (Andreae *et al.*, 2015;
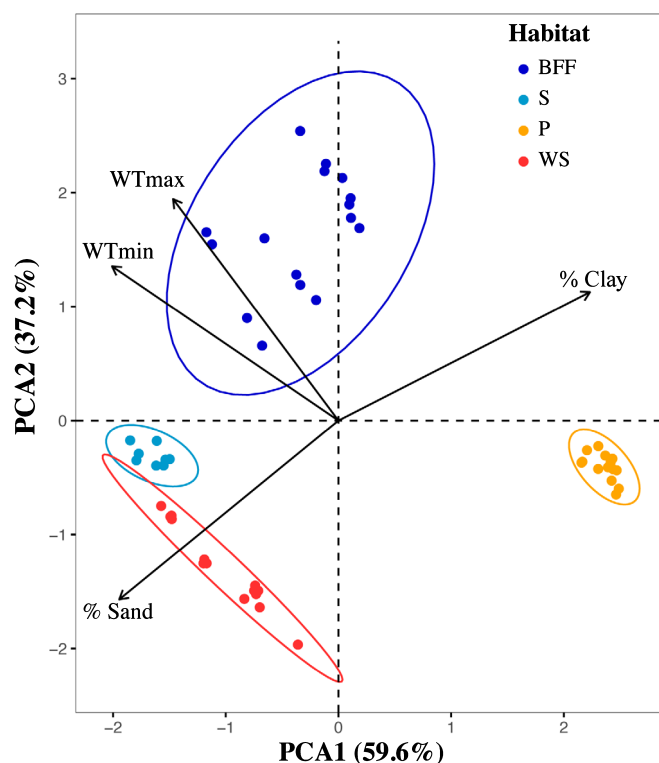
Fig. 2 Principal components analysis (PCA) on soil texture (% Clay and % Sand) and minimum and maximum water table depth (WTmin and WTmax respectively) across the network of 52 forest plots. The first two axes of the PCA account for 96.8% of the total variation among the plots where individuals were sampled. The different colors represent the habitats the trees were collected from. BFF, black-water seasonal floodplain forest; S, swamp forests; P, plateau; WS, white-sand forest.

Targhetta *et al.*, 2015) and ZF-2 reserve (Fig. 1; Fontes *et al.*, 2018a,b). The selected species belong to eight genera (*Couepia, Eperua, Eschweilera, Licania, Pouteria, Protium, Sacoglottis* and *Swartzia*) and six families (Burseraceae, Chrysobalanaceae, Fabaceae, Humiriaceae, Lecythidaceae and Sapotaceae). All trees were sampled during the 2015 dry season (July to September), had DBH between 15 cm and 25 cm, and all branches and leaves were collected 8–15 m above ground. All 16 tree species (Fig. 1) were used to test two hypotheses: (H1) flooded species have higher xylem vulnerability to cavitation compared to non-flooded species; and (H2) hydraulic safety margin among species is similar regardless of environmental water regime. A subset of these species, including three species from three genera (*Eschweilera, Swartzia, Protium*) and one congeneric pair from one other genus (*Licania*; 11 species total; Fig. 1), were used to investigate a third hypothesis (H3) that distant related species in nonflooded habitats have trait values more similar to one another than to closely related species living in flooded habitats. Fifteen of the 16 species are included in the 10 most abundant families in these two regions (Burseraceae, Chrysobalanaceae, Fabaceae, Lecythidaceae and Sapotaceae) and have distributions mostly restricted to one of the four habitats. For the congeneric dataset, we included at least one species from each genus occurring in a flooded (BFF or S) and a nonflooded habitat (P and WS; Fig. 1).

Trait selection

We selected 16 leaf, wood and hydraulic traits that are related to different ecological function such as resource acquisition, defense, mechanical strength, sap transport, xylem vulnerability, and efficiency and safety of the hydraulic system (Table 2).

Stomatal density and specific leaf area Stomatal imprints were obtained by applying clear nail polish on the abaxial surface of fully expanded, mature, and healthy sun leaves. After a 3–5 min drying period, the impressions were peeled off the leaves, placed on microscope slides and embedded in glycerin for examination. Leaf imprints were examined at ×400 magnification using a Leica DM2500 light microscope (Leica Microsystems Vertrieb GmbH, Wetzlar, Germany) and stomatal density (Nstomata) was determined. A digital camera (Nikon digital sight, DS-Fi1) attached to the microscope was used to take a photo of the analyzed impression areas. Three photos/areas per leaf, three leaves per plant and three individual plants per species were examined.

Specific leaf area (SLA) was estimated as the ratio of fresh leaf area to leaf dry mass. Fully expanded, mature and healthy sun leaves were collected between 07:00 h and 09:00 h, and immediately placed in plastic bags with a moist paper towel. Fresh leaf area was measured using a portable leaf area meter (CI-202; CID Inc., Camas, WA, USA) after approx. 2 h of being collected. The leaves were oven-dried at 60°C for 72 h and their dry mass was measured with an analytical balance (0.001 g precision). Three to five individual plants per species (7–10 leaves per tree) were measured.

Carbon (C) and nitrogen (N) isotope composition Leaves were oven dried at 60°C for 72 h and subsequentially ground to a fine powder. Powder of dried leaves was analyzed for N and C stable isotope abundances using elemental analyzer/continuous flow isotope ratio mass spectrometry housed in the Center for Stable Isotope Biogeochemistry at the University of California Berkeley, USA (Exportation permit no. EF2J54U2DM2UQ27Y). Analyses were performed using a CHNOS Elemental Analyzer interfaced to an IsoPrime100 mass spectrometer. Long-term external precision for C and N isotope ratio analyses are $\pm 0.10‰$ and $\pm 0.20‰$, respectively. Measured abundances were denoted as δ values and calculated according to the equation:

$$\delta^{13}C \text{ or } \delta^{15}N = (R_{sample}/R_{standard} - 1) \times 1000[‰].$$

(R_{sample} and $R_{standard}$, ratios of heavy-to-light isotopes of the sample and the respective standard).

Wood specific gravity and xylem anatomy In order to measure the wood specific gravity (WSG), for each tree we collected three branch sections in first order branches (counting from the top) with a diameter of approx. 1 cm and a length of approx. 5 cm. Outer bark and pith > 1 mm in diameter were removed. Branch samples were saturated with water overnight and saturated volume was estimated using the water displacement principle (Williamson & Wiemann, 2010). After measurement of the saturated

Table 2 List of the 16 leaf, wood and hydraulic traits measured for this study and their corresponding abbreviations, units and function.

Trait	Abbreviation	Unit	Function
Leaf			
Stomatal density	Nstomata	μm^{-2}	Resource acquisition
Specific leaf area	SLA	$cm^{-2} g^{-1}$	Resource acquisition and defense
Carbon stable isotope	$\delta^{13}C$	‰	Intrinsic water use efficiency
Nitrogen stable isotope	$\delta^{15}N$	‰	Resource acquisition
Carbon and nitrogen ratio	C : N ratio	$g\,g^{-1}$	Resource acquisition and defense
Wood			
Wood specific gravity	WSG	$g\,cm^{-3}$	Sap conduction, mechanical support and defense
Mean vessel area	VA	μm^2	Sap conduction, efficiency and safety of hydraulic system
Vessel density	VD	μm^{-2}	Sap conduction, efficiency and safety of hydraulic system
Vessel fraction	VF	$\mu m^2 \mu m^{-2}$	Sap conduction, efficiency and safety of hydraulic system
Vessel size to number ratio	S : N ratio	μm^4	Sap conduction, efficiency and safety of hydraulic system
Mean vessel hydraulic diameter	D_{mh}	μm^2	Sap conduction, efficiency and safety of hydraulic system
Hydraulic			
Midday water potential	Ψ_{midday}	MPa	Xylem tension
Water potential when plant lose 50% of its conductivity	P_{50}	MPa	Xylem vulnerability to cavitation
Stem safety margin	SM	MPa	Safety of the hydraulic system
Leaf specific hydraulic conductivity	K_{leaf}	$mmol\,m\,MPa^{-1}\,s^{-1}\,m^{-2}$	Efficiency of the leaf hydraulic system
Stem specific hydraulic conductivity	K_s	$mmol\,m\,MPa^{-1}\,s^{-1}\,m^{-2}$	Efficiency of the stem hydraulic system

volume, samples were dried at 101–105°C for 72 h and dry mass was determined. Branch specific gravity was measured as the dry mass divided by the saturated volume. Three to five plants per species and three branches per plant were measured.

For anatomical trait measurements (Table 2), we collected one branch per tree and three individuals per species from 11 species (three congeneric triplets and one pair). Each branch section was harvested from the last growth unit and had a diameter of 1–2 cm. Branches were placed in plastic vials and stored in a cooler with ice until they were transported to the field station (30 min to 1 h after being collected) where they were frozen for tissue preservation. Before we started the anatomical procedure, samples were slowly thawed in vials with water in a refrigerator overnight. We cut cross-sections (20–30 µm thick) for each branch sample with a rotary microtome (Spencer 820, American Optical, Buffalo, NY). Cross-sections were stained in 0.5% Toluidine Blue for 10 min and rinsed with water. Cross-sections were dehydrated in ethanol series at 50% (for 1 min), at 75% (for 3 min) and at 100% (for 5 min) before mounting. Up to eight cross-sections per sample were embedded in glycerin for histological examination. We selected one cross-section per sample and used a digital camera (Nikon digital sight, DS-Fi1) mounted on a light microscope (Leica DM2500) to shoot three photographs with an APO ×10 lens, covering different parts of the cross-section, allowing the estimation of the variability in vessel size. Image analyses were conducted with IMAGEJ-FIJI4 (Schindelin et al., 2012). For images with good contrast, we performed an automated delimitation of the vessels with a threshold function in FIJI. For those with lower contrast, we filled the vessel areas manually. Anatomical traits measured in the three photographs of each branch sample were then averaged to determine individual values. For each image, we measured individual vessel area (to estimate mean vessel area = VA; μm^2), vessel diameter (D), and counted the total number of vessels per unit area (vessel density = VD; $n\,\mu m^{-2}$). Vessel diameter was estimated as $D = (D_1 + D_2)/2$ (i.e. the mean diameter of an ellipse), where D_1 is the maximum vessel diameter and D_2 is the minimum vessel diameter in µm. We calculated three metrics of hydraulic efficiency, vessel fraction as $V = VA \times VD$; the ratio between size and number of vessels, $S = VA/VD$; and the mean vessel hydraulic diameter (µm), $D_{mh} = (\sum D^4/n)^{1/4}$, where n is the total number of vessels in an image (Zanne et al., 2010; Scholz et al., 2013).

Leaf water potential, hydraulic safety margin, xylem resistance to embolism, leaf and stem hydraulic conductivity Leaf midday water potential (Ψ_{midday}; MPa) was measured at least once a month during the peak of the 2015 dry season (August–October) between 11:30 h and 13:30 h using a pressure chamber (PMS, Corvallis, OR, USA; accurate to 0.05 MPa; Scholander et al., 1965). Three full-developed sun exposed shoots (two to five leaves from the same branches) per plant and three to five plants per species were sampled. Shoots were harvested, immediately wrapped in a damp paper towel, aluminum foil and bagged in separate zip-lock bags with a moist paper towel to avoid further water loss. For each shoot, the assessment of xylem water potential was made c. 5 min after the leaves were collected.

Xylem hydraulic safety margin was calculated as $SM = P_{min} - P_{50}$, where P_{min} is the minimum xylem water potential measured in the field during the dry season of 2015 (August-October). Species' P_{50} was calculated based on Percent Loss of Conductivity curves (PLC or vulnerability curves), by measuring xylem hydraulic conductivity (K) at different xylem water potentials. For each of the 16 species, we collected three sun-exposed branches from three to five individuals. The branches were longer than the maximum vessel length measured for the species. Maximum vessel lengths were measured in a minimum of three individuals per species (Jacobsen et al., 2007) and were in the ranges 29–87 cm in BFF, 46–57 cm in S, 8.5–77 cm

in P and 18–56 cm in WS forests. Different water potentials were obtained using the bench dehydration method (Sperry *et al.*, 1988) and K was measured using an ultra-low-flow meter first proposed by Tyree *et al.* (2002) and adapted by Pereira & Mazzafera (2012). To avoid cutting artifacts: we collected branches at least two-fold longer than the maximum vessel length measured for the species; they were wrapped in dark plastic bags together with wet paper towels for transportation; branches were re-cut under water several times; and branch samples were trimmed with a sharp wood-carving knife as suggested by Beikircher & Mayr (2015). Also, the tension of the branches was relaxed before excising the segment on which measurements were performed. In brief, branches were collected early in the morning (05:30 h– 06:30 h local time), placed in plastic bags to prevent desiccation and transported to the field station 30–60 min after being collected. Branches were bench-dried for different durations (0 min to 3 h) and placed in dark plastic bags for 2–8 h so leaf and xylem water potential would equilibrate. A total of two to three leaves from each branch were used to estimate the water potential. The branches were then recut in water to relax tension in the xylem, ensuring that the final recut sample was still longer than the maximum vessel length. Finally, the branches, longer than the maximum vessel length, were recut under water into five segments (each 4–5 cm long and approx. 1 cm shaved off each end), connected in series to the hydraulic apparatus and initial conductance was measured (Pereira & Mazzafera, 2012). Branches were then flushed for *c.* 25 min at 100 kPa with 20 mM KCl solution, filtered to 0.1-µm (inline filter; GE Water and Process Technologies, Trevose, PA, USA) and vacuum-degassed for ≥ 1 h. After flushing, the maximum conductivity of the same branch segments was assessed. We accounted for the influence of background flow and water temperature (to account for water viscosity change) on all conductance measurements. The PLC was calculated for each of the segments using the hydraulic conductance measurements taken before and after the flushing.

The same apparatus, solution and protocol for branch sampling used to assess hydraulic vulnerability curves (Tyree *et al.*, 2002; Pereira & Mazzafera, 2012) were employed to measure native stem specific hydraulic conductivity and leaf specific conductivity (K_s and K_{leaf}, respectively). To determine K_s and K_{leaf}, we air-collected (branches were not submerged in water before cutting from tree) one branch per tree and three individuals per species from 11 species. Branches $2–3\times$ longer than the maximum vessel length measured were collected at predawn and immediately placed in double plastic bags containing wet tissue paper to minimize post-cutting dehydration. Branches were cut under water, trimmed, connected to the hydraulic apparatus and stem flow was measured (Pereira & Mazzafera, 2012). The length of the branch segments attached to the apparatus was longer than the maximum vessel length measured for the species. K was calculated as the ratio between water flux through the branch segment and the pressure gradient causing that flow (Cruiziat *et al.*, 2002). Hydraulic conductivity (K_h) was calculated as K divided by the cross-section xylem area of the sample. K_s was then calculated as K_h multiplied by sample length (Cruiziat *et al.*, 2002).The distal diameter of these segments varied from 2–4 mm and they were 0.4–1.10 m in length. All leaves located distally from the measured branch were collected and their area was calculated using a portable leaf area meter (CI-202; CID Inc.). K_{leaf} was calculated as K_h divided by the total leaf area of the branch (Venturas *et al.*, 2016).

Statistical analysis

In order to evaluate if species occurring in contrasting habitats differed in their vulnerability to xylem embolism formation (P_{50} values; H1), we used a fixed-effect model. We used a linear mixed-effect model, with species as a random effect on intercept, to test if habitat type affected xylem vulnerability to hydraulic failure (SM values; H2). Student's *t*-test was used to compare the SM values found in this study with the angiosperms' SM global mean (*c.* 0.5 MPa) reported by Choat *et al.* (2012).

In order to investigate if congeneric species from contrasting habitats differed in their leaf, wood and hydraulic traits (H3), we used linear mixed-effect models (genera as a random effect on intercept) to determine the effect of soil texture (clay vs sandy) and water regime (flooded and nonflooded) on species' functional traits. A principal component analysis (PCA) was used to assess the patterns of correlation between traits and to describe hydraulic strategies of species in different habitats. Linear mixed-effect models (species as a random effect on intercept) were used to determine the importance of habitat type on plant's hydraulic strategies (using score values of PCA axes 1 and 2 as the dependent variables). Only the congeneric data (11 species from the genus *Eschweilera*, *Licania*, *Protium* and *Swartzia*) were used in the analyses for testing H3. Only traits that were significantly different between habitats (according to the mixed-effect model results) were used for the PCA-trait analysis.

In order to validate the linear mixed-effect models, we verified visually if residuals were homogeneous and if there was any over-influential observation, using Cook's distance as recommended by Thomas *et al.* (2015). We also checked for normality of the fitted coefficients of the random terms. The residuals of the traits that did not meet the assumptions of a normal distribution (SLA, Ψ_{midday}, P_{50}, VA, VD, S : N ratio, D_{mh}, C : N ratio, K_{leaf} and k_s) were log-transformed before analysis.

We also tested for a phylogenetic signal of all traits using the Blomberg K (Blomberg *et al.*, 2003) and Pagel lambda (Pagel, 1999), with significance tested by 999 permutations. We built a phylogenetic tree for our species using the backbone phylogeny of APG III (R201208029) available in PHYLOMATIC v.3 (Webb & Donoghue, 2005). Branch-lengths were estimated using Grafen's transformation (Grafen, 1992). For all statistical analyses, we used R v.3.3.0 with base packages (R Core Team, 2016).

Results

Species from flooded habitats, such as S and BFF, were significantly more vulnerable to xylem cavitation (47.7% higher P_{50} values) than species from nonflooded habitats (P and WS, $P \leq 0.003$; Fig. 3; Table S2). The only exception was the BFF species *Eschweilera tenuifolia* which had a P_{50} of -2.1 MPa
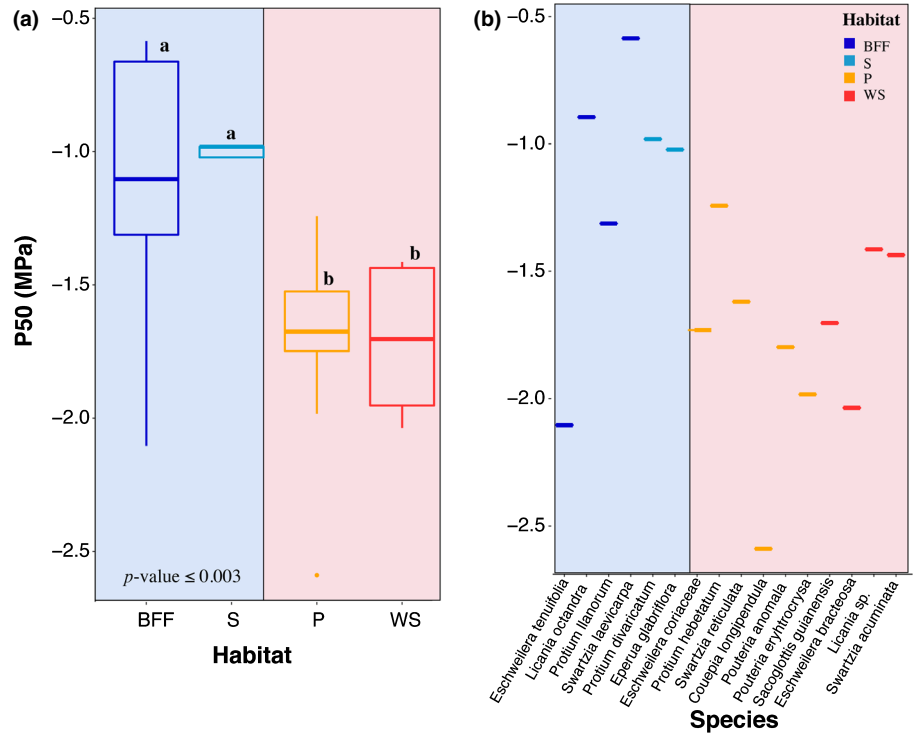
Fig. 3 (a) Boxplot of water potential at 50% loss of xylem hydraulic conductivity (P_{50}) among the different habitats. The lines in the box indicate the mean, and the lines above and below the box indicate the maximum and minimum values respectively. (b) P_{50} values of the 16 studied species. The letters in bold indicate the habitats that had significantly different/similar P_{50} values, according to the linear fixed-effect model results (for a summary of the model's statistical results refer to Supporting Information Table S2). Colors represent the four habitats: dark blue, black-water seasonal floodplain forest (BFF); light blue, swamp forests (S); yellow, plateau (P); and red, white-sand (WS). The blue and red rectangular areas correspond to the flooded and nonflooded habitat, respectively.

(Fig. 3b). These differences in P_{50} values were due mainly to environmental water regime (flooded vs nonflooded) and not specifically to the habitat (BFF, S, P, WS) where the species were found (Fig. 3a; Table S2). Despite the differences in embolism formation between flooded and nonflooded habitats, xylem hydraulic SM across the four habitats were not significantly different ($P = 0.226–0.901$; Fig. 4; Table S3). We also found that all species in this study operated with very narrow (< 1 MPa) SM and were not significantly different from the angiosperms' SM global mean (c. 0.5 MPa) reported by Choat et al. (2012) ($t = -1.41$, df = 46, $P = 0.163$). These results indicate that trees growing in the different Amazonian habitats may be equally likely to cross their P_{50} or P_{88} ($SMP88 = P_{min} - P_{88}$) during extreme droughts.

Species from flooded (BFF and S) and nonflooded habitats (P and WS) showed significant differences in 10 of the 16 leaf, wood and hydraulic traits measured (Fig. 5; Tables S4–S7). These differences were explained primarily by water regime and not by soil texture (Table S4–S7), supporting that water is probably a very important factor shaping species distribution in the Amazon. Flooded habitat species had significantly higher mean values of SLA (33.8%), Nstomata (37.9%), Ψ_{min} (25.75%), P_{50} (46.4%), K_{leaf} (154.6%), K_s (27.1%), VA (39.3%), VF (33.8%) and Dmh (18.7%), whereas species from nonflooded habitats demonstrated higher value of WSG (13.6%; Fig. 5). Vessel density, vessel size: number ratio, xylem SM, leaf C : N ratio, $\delta^{13}C$ and $\delta^{15}N$ did not differ significantly between the congeneric species occurring in the four contrasting habitats (Tables S4–S7). Species mean, minimum and maximum values of the 16 functional traits are shown in Table S8.

The first PCA component explained 40.5% of all variation and was dominated by VA, Dmh, K_{leaf} and P_{50} (Fig. 6a;

Table S9). The second axis accounted for 15% more of the variation and was controlled mainly by WSG, Ψ_{min}, K_s and Nstomata (Fig. 6a; Table S9). Thus, the score of the species on the first axis is a composite of wood anatomical and stem/leaf hydraulic traits where high scores indicate high values of VA, VF, Dmh, K_{leaf} and SLA, and low scores indicate more negative P_{50}. The second axis reflects wood density and resource acquisition. High scores indicate denser wood and higher stomatal density, whereas low values indicate more negative Ψ_{min}, and higher values of K_s. Flooded habitat species (BFF and S) mostly were grouped on the right side of the PCA space (Fig. 6a–c; Table S10), with the exception of the species E. tenuifolia which is found in BFF but has a high vulnerability to xylem embolism. By contrast, species from nonflooded habitats (P and WS) were located on the left side of the PCA space (Fig. 6; Table S10). Water regime was the main environmental driver explaining this pattern of species distribution along axis 1 of the PCA space (Fig. 6b; Table S10). Furthermore, this pattern was driven mainly by hydraulic and anatomical traits that are related with water transport, corroborating the importance of water availability for species distribution among habitats in the tropics.

Finally, there was no phylogenetic signal for any of the 16 traits analyzed in this study (K ranged from 0.18 to 0.43, and λ from 0.01 to 0.57; Table S11), indicating that these traits are not conserved in the phylogeny. These results show that unrelated species from flooded habitats are more similar to each other than they are to their congeners growing in drier (nonflooded) habitats.

Discussion

Our study reveals that xylem embolism resistance varies significantly between flooded and nonflooded habitats at small (swamp
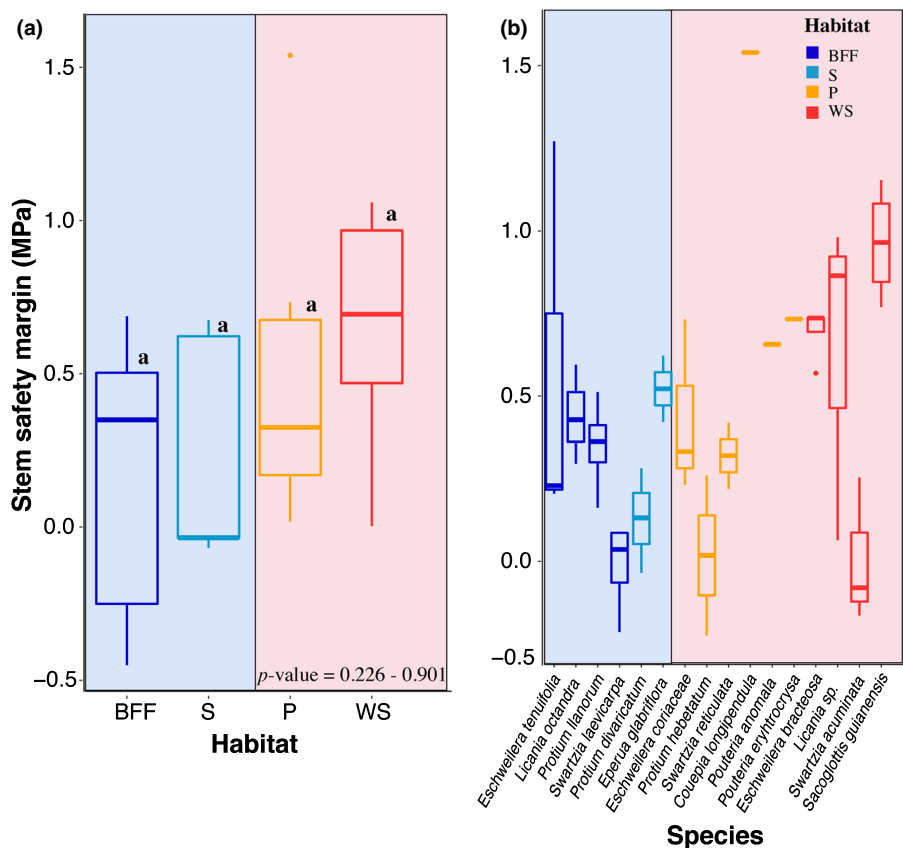
Fig. 4 (a) Boxplot of stem hydraulic safety margin ($SM = P_{min} - P_{50}$) among the different habitats. The lines in the box indicate the mean, and the lines above and below the box indicate the maximum and minimum values respectively. (b) SMs of the 16 studied species. The letters in bold indicate that the four habitats did not have significantly different SM values, according to the linear mixed-effect model results (for a summary of the model's statistical results refer to Supporting information Table S3). Colors represent the four habitats: dark blue, black-water seasonal floodplain forest (BFF); light blue, swamp forests (S); yellow, plateau (P); and red, white-sand (WS). The blue and red rectangular areas correspond to the flooded and nonflooded habitat, respectively.

(S) vs plateau (P)) and regional (P/white-sand forests (WS) vs. S/black-water seasonal floodplain forest (BFF)) spatial scales within four Amazonian habitats. Species growing in nonflooded habitats are more resistant to cavitation, but they also experience a more negative minimum water potential than those growing in flooded habitats. Thus, all of the tree species in our sample were found to operate within narrow safety margins (SM; < 1 MPa), and were not significantly different from the angiosperms' SM global mean (Choat *et al.*, 2012), indicating that all studied species may be equally likely to cross their P_{50} (the water potential at which plants lose 50% of their hydraulic conductivity) during drought events. We also found that congeneric species did not converge in multidimensional trait-space based on their leaf, wood or hydraulic traits. Instead, species from flooded habitats (BFF and S) were more functionally similar to one another than to their congeneric species growing in the adjacent nonflooded habitats (P and WS), showing a pattern of convergent evolution. Furthermore, we found that water regime was more important in determining forest trait composition than soil texture. Our results suggest that these differences evolved repeatedly and independently in each genus due to habitat-mediated speciation.

Embolism resistance and hydraulic safety margins

We found that species from nonflooded habitats have significantly lower P_{50} values than their congeneric species growing in flooded habitats (Fig. 3). This result supports the idea of an increase in xylem cavitation resistance with declining water availability (Santiago *et al.*, 2018; Oliveira *et al.*, 2019). Low values of P_{50} indicate high xylem safety and they are frequently used to compare different species' vulnerability to water deficit (e.g. Powell *et al.*, 2017; Santiago *et al.*, 2018; Oliveira *et al.*, 2019). In S and BFF habitats, the water table is close to or even above the surface, suggesting that plants are not water-limited during the dry season. Because it is energetically costly to build wood and leaf tissues that are resistant to water deficit (higher carbon (C) needed per unit sapwood area growth; van Gelder *et al.*, 2006; Sobrado, 2009), it may not be advantageous for species growing in flooded habitats to invest in a safer hydraulic system. Thus, plants that have a greater maximum hydraulic conductivity may be stronger competitors in these habitats, whereas trees that have slow resource acquisition characteristics may be selected against or outcompeted from these wet environments (Chapin, 1991; Reich, 2014). By contrast, species in P and WS areas must cope with lower water availability, and water stress may be a key environmental filter in these habitats. Furthermore, the four studied habitats have similar atmospheric water demand and thus, soil water regime most likely has a filtering effect, selecting plants whose xylem can tolerate more negative water potentials.

However, P_{50} values only provide information about the water potential at which plants lose 50% of their hydraulic conductivity due to xylem cavitation (Bucci et al., 2016; Santiago *et al.*, 2018). Thus, xylem hydraulic safety margin data ($SM = P_{min} - P_{50}$) may be more informative than only documenting P_{50} because SMs indicate how close a plant operates to the loss of its hydraulic capacity (Meinzer *et al.*, 2009; Bucci *et al.*, 2016; Ziegler *et al.*,
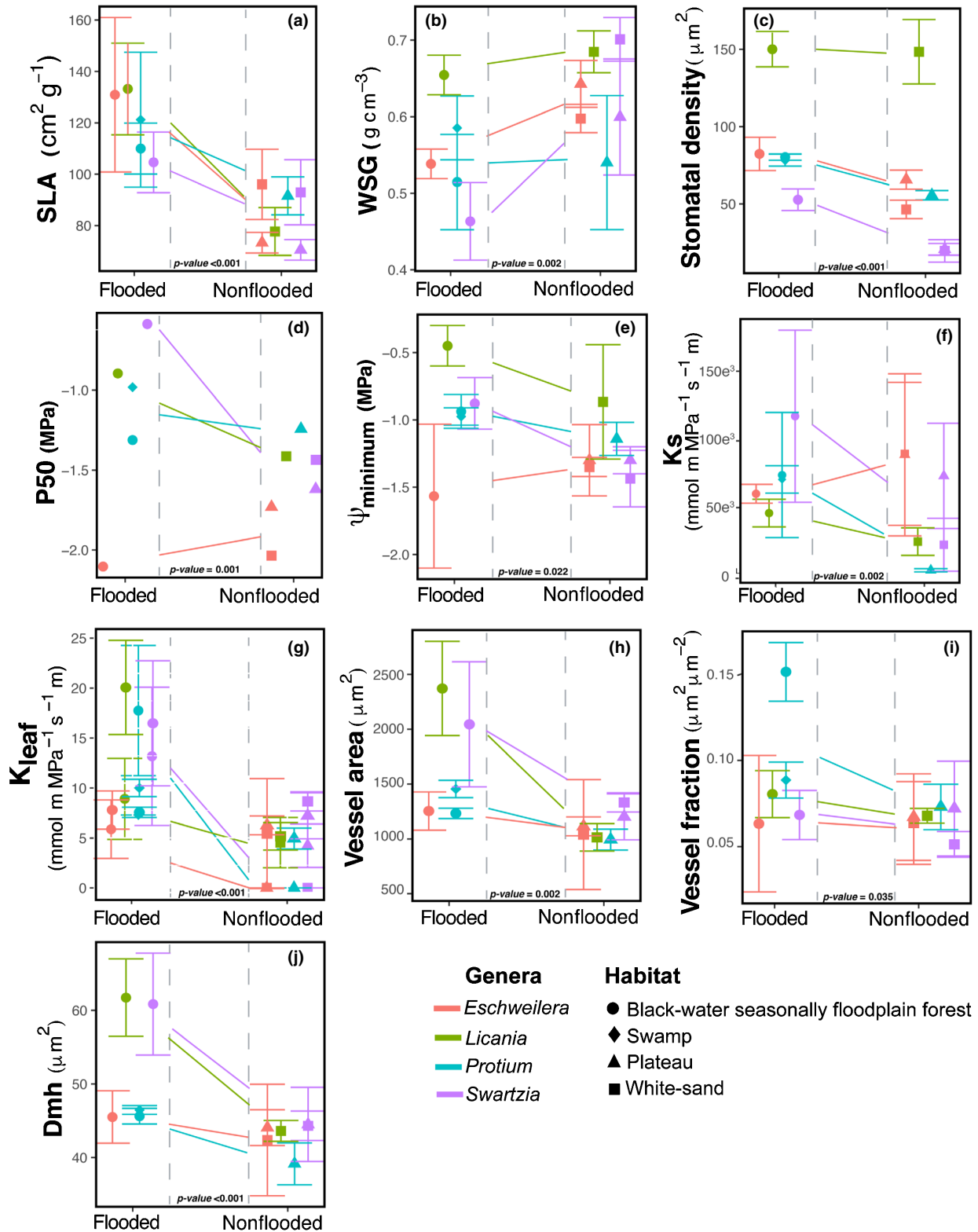
Fig. 5 (a) Specific leaf area, (b) wood specific gravity, (c) stomatal density, (d) water potential at 50% loss of hydraulic conductivity, (e) midday water potential, (f) xylem specific hydraulic conductivity, (g) leaf specific hydraulic conductivity, (h) mean vessel area (VA), (i) mean vessel fraction, and (j) mean vessel hydraulic diameter for three triplets (*Eschweilera*, *Protium*, and *Swartzia*) and one pair (*Licania*) of congeneric species associated with two flooded (black-water seasonal floodplain forest, and swamp), and two nonflooded habitats (plateau and white-sand forest). Different line colors connect mean trait values of the different congeneric species occurring in habitats that differ in water regime. Only traits that had a significant relationship ($P < 0.05$) based on the results of the mixed-effect linear model are shown here. Soil texture did not explain any of the trait values measured in this study. All relationships are shown in original measurement units, but for the mixed-effect linear model analyses we used log-transformed values of SLA, Ψ_{midday}, P_{50}, K_s, K_{leaf}, VA and D_{mh}, to achieve normality. Refer to Supporting information Tables S4–S8 for a statistical summary of the models' results.
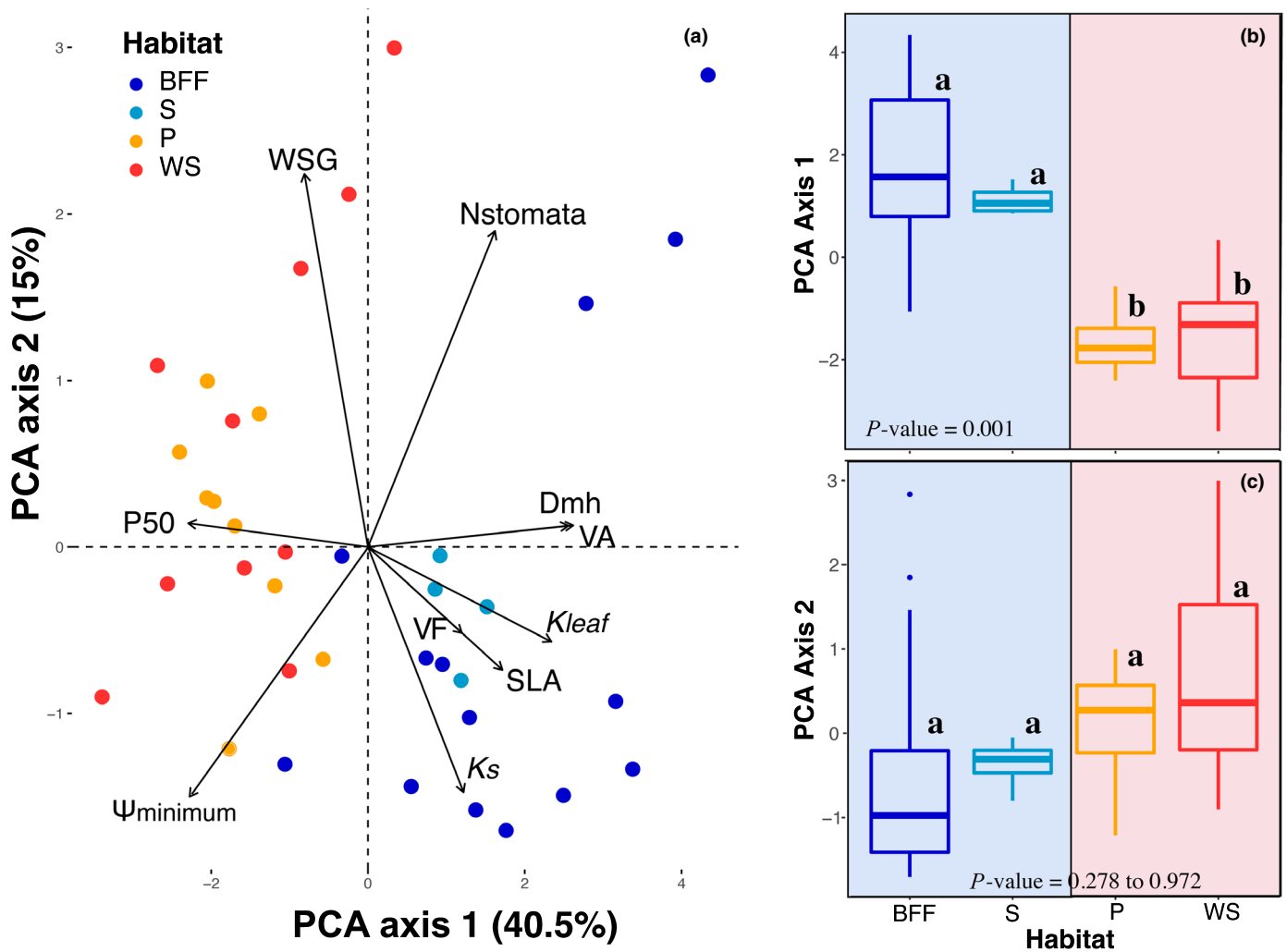
Fig. 6 (a) Principal components analysis (PCA) of the 37 individuals, belonging to 11 tree species. Only the 10 traits that had a significant relationship ($P < 0.05$) based on the mixed-effect linear model results (Supporting information Tables S4–S8) were used for PCA analysis. WSG, wood specific gravity (g cm^{-3}); Nstomata, stomatal density; $\Psi_{minimum}$, minimum water potential measured in the hottest part of the day; VA, mean vessel area; D_{mh}, mean vessel hydraulic diameter; P_{50}, water potential when 50% of xylem conductivity is lost; SLA, specific leaf area; VF, mean vessel fraction; K_{leaf}, leaf specific hydraulic conductivity; and K_s, stem specific hydraulic conductivity. (b) Boxplot of values of PCA axis 1 among the four different habitats. (c) Boxplot of values of PCA axis 2 among the four different habitats. The letters in bold indicate the habitats that had significantly different/similar PCA scores values, according to the linear mixed-effect model results (Table S10). Colors represent the four habitats: dark blue, black-water seasonal floodplain forest (BFF); light blue, swamp forests (S); yellow, plateau (P); and red, white-sand (WS). The blue and red rectangular areas correspond to the flooded and nonflooded habitat, respectively.

2019). Indeed, we found that despite the differences in vulnerability to embolism between flooded and nonflooded habitats (Fig. 3), SMs across the four habitats were not significantly distinct and were independent of water regime or soil texture (Fig. 4). These results indicate that species from flooded and nonflooded habitats evolved to optimize their water transport system, having little room to accommodate for anomalous climate conditions and, thus, may be as likely to experience hydraulic failure during severe droughts.

We found that some species from BFF (*Swartzia laevicarpa*), P (*Protium hebetatum*) and WS (*Swartzia acuminata*) were operating under negative safety margins (with <50% of their hydraulic conductivity; Fig. 4), suggesting that these species were experiencing some degree of water stress during the time

of data collection. During our study, the most severe drought registered in the last decade occurred in the Central Amazon, with profound effects on plant physiological performance (Fontes *et al.*, 2018b). Our results indicate that this drought amplified the degree of physiological stress in trees across Amazonian habitats, further reiterating how species from flooded and nonflooded habitats may be impacted in a similar way by changes in climate. These results are particularly important because Amazonian trees may have limited capacity to acclimate plant hydraulic properties in response to long-term drought (Bittencourt *et al.*, 2020). However, more research on the patterns of xylem vulnerability and SMs across the different habitats in the Amazon is needed before broad conclusions can be made.

Leaf, wood and hydraulic traits across contrasting Amazonian habitats

We found strong trait variation between flooded (BFF and S) and nonflooded (P and WS) Amazonian habitats. Species from P and WS forests were more functionally similar to each other than to their congeneric species growing in neighboring BFF or S areas. This result was surprising, especially because WS and P forests are very different habitats and therefore could be expected to select for very different hydraulic strategies. Plateau soils have much higher clay fraction, compared to Brazilian WS, have higher nutrient availability, trees are taller (canopy height approx. 30 m), and the understory has lower solar radiation and higher relative humidity (Fine *et al.*, 2006; Baraloto *et al.*, 2011; Stropp *et al.*, 2011, 2014; Fortunel *et al.*, 2012; Damasco *et al.*, 2013). Thus, the fact that P and WS forests were not significantly different in any of the hydraulic traits measured in this study reinforces the idea that water regime, specially access to groundwater, can be a strong predictor of species hydraulic functional composition (Fortunel *et al.*, 2013; Cosme *et al.*, 2017; Chitra-Tarak *et al.*, 2018; Medeiros *et al.*, 2019).

Species from nonflooded habitats had a higher leaf mass per unit area (lower SLA) and higher wood specific gravity (denser wood) than their congeneric species from flooded areas (Fig. 5a, b). These results suggest that nonflooded habitat species may invest more in tissue quality to enhance the retention of captured resources, protection against herbivores, mechanical strength and/or longer leaf lifespans (Reich *et al.*, 1997; Westoby, 1998; Fortunel *et al.*, 2013; Kunstler *et al.*, 2016) than their congeneric species from flooded habitats. In contrast, species from flooded areas had a larger vessel area and wider vessel hydraulic diameters (Fig. 5h,j). Wider vessels can transport water, oxygen and nutrients more efficiently, and allow plants to achieve higher maximum hydraulic conductivity; however, it also can make them more vulnerable to water stress (higher risk of xylem cavitation; Fig. 5c–h; Sperry *et al.*, 2006; Gleason *et al.*, 2016; Hacke *et al.*, 2017). Neither VD, vessel size (S) : number (N) ratio, xylem SM, leaf C : nitrogen (N) ratio, $\delta^{13}C$ nor $\delta^{15}N$ differed significantly between the congeneric species occurring in the four contrasting environments (Tables S4–S7). These results are consistent with the findings of Cosme *et al.*(2017) who reported similar trait combinations for species associated with swamp (valley) vs plateau forests. Therefore, our results suggest that species from the studied flooded Amazonian habitats have a tendency towards 'fast-resource-acquisition strategies', *sensu* Reich (2014), whereas trees in the nonflooded areas have traits that enhance resistance and resource conservation.

We acknowledge that the traits measured in this study may not represent all of the most important traits underlying habitat partitioning (Fortunel *et al.*, 2013; Fortunel *et al.*, 2014; Díaz *et al.*, 2016; Cosme *et al.*, 2017). However, we were able to detect a combination of traits that could restrict flooded habitat species from establishing in nonflooded areas of the Amazon forest. Also, our study provides further evidence that tropical tree communities are not randomly assembled. Instead, niche-based processes, such as competition and environmental filtering, are key

processes shaping community assemblage in these megadiverse systems (Baraloto *et al.*, 2012; Fortunel *et al.*, 2013; Cosme *et al.*, 2017; Oliveira *et al.*, 2019). All of the wood, leaf and hydraulic traits that we measured showed strong signals of convergent evolution to environmental drivers rather than phylogenetic conservatism. Thus, functional traits within flooded vs nonflooded environments in the Amazon are similar in unrelated tree species, and these trait combinations have either evolved repeatedly and independently across many different phylogenetic lineages or adjusted morphologically (through plasticity) to the local environment. These patterns can be explained by convergent evolution in functional traits along life-history trade-off axes, in combination with local environmental sorting processes (Fortunel *et al.*, 2013; Gleason *et al.*, 2016; Leibold & Chase, 2017). Moreover, the different environmental conditions found in the Amazon may be a key factor in promoting local speciation by imposing strong environmental selective pressure in local populations (Leibold & Chase, 2017). Other studies have pointed out that habitat specialists in the Amazonian flora have evolved multiple times in many different lineages (e.g. Fine & Baraloto, 2016). Here, we provide empirical results showing that one important mechanism to explain how habitat specialization evolves, is likely related to hydraulic traits measured in our study. Moreover, the fact that species within the genera which we studied are restricted to only a subset of the four major habitats, strongly suggests that hydraulic traits are labile but become fixed at the species level, probably due to the trade-offs inherent in being successful in a flooded or nonflooded habitat. Such habitat-mediated trade-offs would select against intermediate phenotypes, driving the evolution of habitat-specific hydraulic traits. In addition, phenotypic plasticity in hydraulic traits is unlikely to be an alternative strategy because we find such consistent patterns among unrelated plant lineages.

Much of the variation that we found in hydraulic and anatomical traits was related with PCA axis 1, which was also the axis responsible for the clear separation between flooded and nonflooded habitats in the PCA space (Fig. 6). These results highlight the importance of hydraulic-related traits in species segregation among the habitats and have strong implications for modeling tropical species response to changes in climate. Recently, newer models such as TFS-Hydro (Christoffersen *et al.*, 2016), Community Land Model v.5 (CLM5) and Ecosystem Demography model 2 (ED2; Xu *et al.*, 2016) have incorporated plant hydraulic traits, making substantial improvements in the predictions of vegetation response to changes in temperature and water availability (Anderegg *et al.*, 2016; Eller *et al.*, 2018).

To the best of our knowledge, the present study is the first to assess plant anatomical (e.g. mean vessel hydraulic diameter (D_{mh}) and vessel area (VA)) and hydraulic traits (e.g. P_{50}, SM, specific hydraulic conductivity and leaf specific conductivity (K_s and K_{leaf})) in the four main forested habitats of the Amazon Basin. We show for the first time that, based on their SM values, trees from flooded and nonflooded habitats may be impacted in a similar way by future drought events and that water regime at local scales is important for explaining trait variability in Amazonian forests. Although such findings help us understand the

processes shaping community assemblages in the tropics, further challenges remain. An exciting and expanding area of study is the role of trait plasticity and acclimation in species survival in dryer and warmer conditions (e.g. Drake *et al.*, 2018). Also, studies like the one presented here would benefit by adding similar data and analyses from reciprocal transplant experiments among the contrasting Amazonian habitats to test for local adaptation in tropical tree species' lineages (e.g. Fine *et al.*, 2006; Fortunel *et al.*, 2016). Finally, understanding how hydraulic traits vary among habitats (locally and regionally) combined with an improved understanding of their role in species distribution will improve our ability to accurately predict how plant communities in the Amazon will be impacted by future climatic events.

Author contributions

CGF, PVAF, TED and JQC planned and designed the research; CFG performed measurements and conducted fieldwork; CFG performed statistical analyses and wrote the manuscript; CFG, PVAF, PRLB, FW, NH, MTFP, JQC and TED revised and provided comments on the manuscript; and FW, NH, MTFP and JQC provided financial and/or logistical support.

ORCID

Paulo R. L. Bittencourt (iD) https://orcid.org/0000-0002-1618-9077
Jeffrey Q. Chambers (iD) https://orcid.org/0000-0003-3983-7847
Todd E. Dawson (iD) https://orcid.org/0000-0002-6871-3440
Paul V. A. Fine (iD) https://orcid.org/0000-0002-0550-5628
Clarissa G. Fontes (iD) https://orcid.org/0000-0003-4712-3764
Niro Higuchi (iD) https://orcid.org/0000-0002-1203-4502
Maria Teresa Fernandez Piedade (iD) https://orcid.org/0000-0002-7320-0498
Florian Wittmann (iD) https://orcid.org/0000-0001-9180-356X

References

Adeney JM, Christensen NL, Vicentini A, Cohn-Haft M. 2016. White-sand ecosystems in Amazonia. *Biotropica* **48**: 7–23.

Anderegg WR, Klein T, Bartlett M, Sack L, Pellegrini AF, Choat B, Jansen S. 2016. Meta-analysis reveals that hydraulic traits explain cross-species patterns of drought-induced tree mortality across the globe. *Proceedings of the National Academy of Sciences, USA* **113**: 5024–5029.

Andreae M, Acevedo O, Araùjo A, Artaxo P, Barbosa C, Barbosa H, Brito J, Carbone S, Chi X, Cintra B et al. 2015. The Amazon Tall Tower Observatory (ATTO): overview of pilot measurements on ecosystem ecology, meteorology, trace gases, and aerosols. *Atmospheric Chemistry and Physics* **15**: 10723–10776.

Assis RL, Wittmann F, Piedade MTF, Haugaasen T. 2015. Effects of hydroperiod and substrate properties on tree alpha diversity and composition in Amazonian floodplain forests. *Plant Ecology* **216**: 41–54.

Baraloto C, Hardy OJ, Paine C, Dexter KG, Cruaud C, Dunning LT, Gonzalez MA, Molino JF, Sabatier D, Savolainen V et al. 2012. Using functional traits and phylogenetic trees to examine the assembly of tropical tree communities. *Journal of Ecology* **100**: 690–701.

Baraloto C, Rabaud S, Molto Q, Blanc L, Fortunel C, Herault B, Davila N, Mesones I, Rios M, Valderrama E. 2011. Disentangling stand and environmental correlates of aboveground biomass in Amazonian forests. *Global Change Biology* **17**: 2677–2688.

Beikircher B, Mayr S. 2015. Avoidance of harvesting and sampling artefacts in hydraulic analyses: a protocol tested on Malus domestica. *Tree Physiology* **36**: 797–803.

Bittencourt PRL, Oliveira RS, da Costa ACL, Giles AL, Coughlin I, Costa PB, Bartholomew DC, Ferreira LV, Vasconcelos SS, Barros FV. 2020. Amazonian trees have limited capacity to acclimate plant hydraulic properties in response to long-term drought. *Global Change Biology* 1–16. doi: 10.1111/gcb.15040.

Blackman CJ, Gleason SM, Chang Y, Cook AM, Laws C, Westoby M. 2014. Leaf hydraulic vulnerability to drought is linked to site water availability across a broad range of species and climates. *Annals of botany* **114**: 435–440.

Blomberg SP, Garland T Jr, Ives AR. 2003. Testing for phylogenetic signal in comparative data: behavioral traits are more labile. *Evolution* **57**: 717–745.

Bonal D, Burban B, Stahl C, Wagner F, Hérault B. 2016. The response of tropical rainforests to drought—lessons from recent research and future prospects. *Annals of Forest Science* **73**: 27–44.

Bucci SJ, Goldstein G, Scholz FG, Meinzer FC. 2016. Physiological significance of hydraulic segmentation, nocturnal transpiration and capacitance in tropical trees: Paradigms revisited. In: Goldstein G, Santiago L, eds. *Tropical tree physiology. Tree physiology 6.* Cham: Springer.

Chapin FS. 1991. Integrated responses of plants to stress. *BioScience* **41**: 29–36.

Chitra-Tarak R, Ruiz L, Dattaraja HS, Mohan Kumar MS, Riotte J, Suresh HS, McMahon SM, Sukumar R. 2018. The roots of the drought: Hydrology and water uptake strategies mediate forest-wide demographic response to precipitation. *Journal of Ecology* **106**: 1495–1507.

Choat B, Jansen S, Brodribb TJ, Cochard H, Delzon S, Bhaskar R, Bucci SJ, Feild TS, Gleason SM, Hacke UG et al. 2012. Global convergence in the vulnerability of forests to drought. *Nature* **491**: 752–755.

Christoffersen BO, Gloor M, Fauset S, Fyllas NM, Galbraith DR, Baker TR, Kruijt B, Rowland L, Fisher RA, Binks OJ. 2016. Linking hydraulic traits to tropical forest function in a size-structured and trait-driven model (TFS v. 1-Hydro). *Geoscientific Model Development* **9**: 4227.

Connell JH. 1978. Diversity in tropical rain forests and coral reefs. *Science* **199**: 1302–1310.

Cosme LH, Schietti J, Costa FR, Oliveira RS. 2017. The importance of hydraulic architecture to the distribution patterns of trees in a central Amazonian forest. *New Phytologist* **215**: 113–125.

Cruiziat P, Cochard H, Amglio T. 2002. Hydraulic architecture of trees: main concepts and results. *Annals of Forest Science* **59**: 723–752.

Damasco G, Vicentini A, Castilho CV, Pimentel TP, Nascimento HE. 2013. Disentangling the role of edaphic variability, flooding regime and topography of Amazonian white-sand vegetation. *Journal of Vegetation Science* **24**: 384–394.

Díaz S, Kattge J, Cornelissen JH, Wright IJ, Lavorel S, Dray S, Reu B, Kleyer M, Wirth C, Prentice IC *et al.* 2016. The global spectrum of plant form and function. *Nature* 529: 167.

Doughty CE, Goulden ML. 2008. Are tropical forests near a high temperature threshold? *Journal of Geophysical Research: Biogeosciences* 113: 1–12.

Drake JE, Tjoelker MG, Vårhammar A, Medlyn BE, Reich PB, Leigh A, Pfautsch S, Blackman CJ, López R, Aspinwall MJ *et al.* 2018. Trees tolerate an extreme heatwave via sustained transpirational cooling and increased leaf thermal tolerance. *Global Change Biology* 24: 2390–2402.

Eller CB, Rowland L, Oliveira RS, Bittencourt PRL, Barros FV, da Costa ACL, Meir P, Friend AD, Mencuccini M, Sitch S. 2018. Modelling tropical forest responses to drought and El Niño with a stomatal optimization model based on xylem hydraulics. *Philosophical Transactions of the Royal Society of London. Series B: Biological Sciences* 373: 20170315.

Engelbrecht BM, Comita LS, Condit R, Kursar TA, Tyree MT, Turner BL, Hubbell SP. 2007. Drought sensitivity shapes species distribution patterns in tropical forests. *Nature* 447: 80–82.

Ferraz J, Ohta S, Sales Pd. 1998. Distribuição dos solos ao longo de dois transectos em floresta primária ao norte de Manaus (AM). In: Higuchi N, Campos MAA, Sampaio PTB, Santos J, eds. *Pesquisas Florestais para a Conservação da Floresta e Reabilitação de Áreas Degradadas da Amazônia.* Manaus, Amazonas: Instituto Nacional de Pesquisas da Amazônia, 110–143.

Fine PV. 2015. Ecological and evolutionary drivers of geographic variation in species diversity. *Annual Review of Ecology, Evolution, and Systematics* 46: 369–392.

Fine PV, Baraloto C. 2016. Habitat endemism in white-sand forests: insights into the mechanisms of lineage diversification and community assembly of the Neotropical flora. *Biotropica* 48: 24–33.

Fine PV, Kembel SW. 2011. Phylogenetic community structure and phylogenetic turnover across space and edaphic gradients in western Amazonian tree communities. *Ecography* 34: 552–565.

Fine PV, Miller ZJ, Mesones I, Irazuzta S, Appel HM, Stevens MHH, Sääksjärvi I, Schultz JC, Coley PD. 2006. The growth–defense trade-off and habitat specialization by plants in Amazonian forests. *Ecology* 87: S150–S162.

Fontes CG, Chambers JQ, Higuchi N. 2018a. Revealing the causes and temporal distribution of tree mortality in Central Amazonia. *Forest Ecology and Management* 424: 177–183.

Fontes CG, Dawson TE, Jardine K, McDowell N, Gimenez BO, Anderegg L, Negrón-Juárez R, Higuchi N, Fine PV, Araújo AC. 2018b. Dry and hot: the hydraulic consequences of a climate change–type drought for Amazonian trees. *Philosophical Transactions of the Royal Society of London. Series B: Biological Sciences* 373: 20180209.

Fortunel C, Fine PVA, Baraloto C, Dalling J. 2012. Leaf, stem and root tissue strategies across 758 Neotropical tree species. *Functional Ecology* 26(5): 1153–1161.

Fortunel C, Paine CET, Fine PVA, Kraft NJB, Baraloto C, De Deyn G. 2014. Environmental factors predict community functional composition in Amazonian forests. *Journal of Ecology* 102: 145–155.

Fortunel C, Paine CT, Fine PV, Mesones I, Goret JY, Burban B, Cazal J, Baraloto C. 2016. There's no place like home: seedling mortality contributes to the habitat specialisation of tree species across Amazonia. *Ecology Letters* 19: 1256–1266.

Fortunel C, Ruelle J, Beauchene J, Fine PV, Baraloto C. 2013. Wood specific gravity and anatomy of branches and roots in 113 Amazonian rainforest tree species across environmental gradients. *New Phytologist* 202: 79–94.

Fu R, Yin L, Li W, Arias PA, Dickinson RE, Huang L, Chakraborty S, Fernandes K, Liebmann B, Fisher R *et al.* 2013. Increased dry-season length over southern Amazonia in recent decades and its implication for future climate projection. *Proceedings of the National Academy of Sciences, USA* 110: 18110–18115.

van Gelder H, Poorter L, Sterck F. 2006. Wood mechanics, allometry, and life-history variation in a tropical rain forest tree community. *New Phytologist* 171: 367–378.

Gleason SM, Westoby M, Jansen S, Choat B, Hacke UG, Pratt RB, Bhaskar R, Brodribb TJ, Bucci SJ, Cao KF *et al.* 2016. Weak tradeoff between xylem safety and xylem-specific hydraulic efficiency across the world's woody plant species. *New Phytologist* 209: 123–136.

Grafen A. 1992. The uniqueness of the phylogenetic regression. *Journal of Theoretical Biology* 156: 405–423.

Hacke UG, Spicer R, Schreiber SG, Plavcová L. 2017. An ecophysiological and developmental perspective on variation in vessel diameter. *Plant, Cell & Environment* 40: 831–845.

Jacobsen AL, Pratt RB, Davis SD, Ewers FW. 2007. Cavitation resistance and seasonal hydraulics differ among three arid Californian plant communities. *Plant, Cell & Environment* 30: 1599–1609.

Klein T, Yakir D, Buchmann N, Grünzweig JM. 2014. Towards an advanced assessment of the hydrological vulnerability of forests to climate change-induced drought. *New Phytologist* 201: 712–716.

Kunert N, Aparecido LMT, Wolff S, Higuchi N, dos Santos J, de Araujo AC, Trumbore S. 2017. A revised hydrological model for the Central Amazon: the importance of emergent canopy trees in the forest water budget. *Agricultural and Forest Meteorology* 239: 47–57.

Kunstler G, Falster D, Coomes DA, Hui F, Kooyman RM, Laughlin DC, Poorter L, Vanderwel M, Vieilledent G, Wright SJ *et al.* 2016. Plant functional traits have globally consistent effects on competition. *Nature* 529: 204.

Leibold MA, Chase JM. 2017. *Metacommunity ecology.* Princeton, NJ, USA: Princeton University Press.

Marengo JA, Souza CA, Thonicke K, Burton C, Halladay K, Betts RA, Soares WR. 2018. Changes in climate and land use over the Amazon Region: current and future variability and trends. *Frontiers in Earth Science* 6: 228.

Marengo JA, Tomasella J, Alves LM, Soares WR, Rodriguez DA. 2011. The drought of 2010 in the context of historical droughts in the Amazon region. *Geophysical Research Letters* 38: 1–5. https://doi.org/10.1029/2011GL047436.

Medeiros CD, Scoffoni C, John GP, Bartlett MK, Inman-Narahari F, Ostertag R, Cordell S, Giardina C, Sack L. 2019. An extensive suite of functional traits distinguishes Hawaiian wet and dry forests and enables prediction of species vital rates. *Functional Ecology* 33: 712–734.

Medina E, Sobrado M, Herrera R. 1978. Significance of leaf orientation for leaf temperature in an Amazonian sclerophyll vegetation. *Radiation and Environmental Biophysics* 15: 131–140.

Meinzer FC, Johnson DM, Lachenbruch B, McCulloh KA, Woodruff DR. 2009. Xylem hydraulic safety margins in woody plants: coordination of stomatal control of xylem tension with hydraulic capacitance. *Functional Ecology* 23: 922–930.

Oliveira RS, Costa FR, van Baalen E, de Jonge A, Bittencourt PR, Almanza Y, Barros FdV, Cordoba EC, Fagundes MV, Garcia S. 2019. Embolism resistance drives the distribution of Amazonian rainforest tree species along hydro-topographic gradients. *New Phytologist* 221: 1457–1465.

Pagel M. 1999. Inferring the historical patterns of biological evolution. *Nature* 401: 877.

Parolin P, Wittmann F. 2010. Struggle in the flood: tree responses to flooding stress in four tropical floodplain systems. *AoB Plants* 2010: 1–19.

Pereira L, Mazzafera P. 2012. A low cost apparatus for measuring the xylem hydraulic conductance in plants. *Bragantia* 71: 583–587.

Phillips OL, Vargas PN, Monteagudo AL, Cruz AP, Zans MEC, Sánchez WG, Yli-Halla M, Rose S. 2003. Habitat association among Amazonian tree species: a landscape-scale approach. *Journal of Ecology* 91: 757–775.

Powell TL, Wheeler JK, de Oliveira AAR, da Costa ACL, Saleska SR, Meir P, Moorcroft PR. 2017. Differences in xylem and leaf hydraulic traits explain differences in drought tolerance among mature Amazon rainforest trees. *Global Change Biology* 23: 4280–4293.

R Core Team. 2016. *R: A language and environment for statistical com-puting.* Vienna, Austria: R Foundation for Statistical Computing. [WWW document] URL https://www.R-project.org/.

Reich PB. 2014. The world-wide 'fast-slow' plant economics spectrum: a traits manifesto. *Journal of Ecology* 102: 275–301.

Reich PB, Walters MB, Ellsworth DS. 1997. From tropics to tundra: global convergence in plant functioning. *Proceedings of the National Academy of Sciences, USA* 94: 13730–13734.

Ribeiro J, Hopkins M, Vicentini A, Sothers C, Costa MdS, Brito Jd, Souza Md, Martins L, Lohmann L, Assunção P. 1999. *Flora da reserva Ducke: Flora da reserva Ducke: Flora da reserva Ducke: guia de identificação de plantas vasculares*

de uma floresta de terra-firme na Amazônia Central. Manaus, Amazonas: Instituto Nacional de Pesquisas da Amazônia.

Rinne H, Guenther A, Greenberg J, Harley P. 2002. Isoprene and monoterpene fluxes measured above Amazonian rainforest and their dependence on light and temperature. *Atmospheric Environment* **36**: 2421–2426.

Roberts J, Cabral OM, Costa Jd, McWilliam A, Sá TdA. 1996. An overview of the leaf area index and physiological measurements during ABRACOS. In: Gash JHC, Nobre CA, Roberts JM, Victoria RL, eds. *Amazonian deforestation and climate.* Chichester, UK: John Wiley & Sons.

Saatchi SS, Houghton RA, Dos Santos Alvaláá RC, Soares JV, Yu Y. 2007. Distribution of aboveground live biomass in the Amazon basin. *Global Change Biology* **13**: 816–837.

Santiago LS, De Guzman ME, Baraloto C, Vogenberg JE, Brodie M, Hérault B, Fortunel C, Bonal D. 2018. Coordination and trade-offs among hydraulic safety, efficiency and drought avoidance traits in Amazonian rainforest canopy tree species. *New Phytologist* **218**: 1015–1024.

Schietti J, Emilio T, Rennó CD, Drucker DP, Costa FR, Nogueira A, Baccaro FB, Figueiredo F, Castilho CV, Kinupp V. 2014. Vertical distance from drainage drives floristic composition changes in an Amazonian rainforest. *Plant Ecology & Diversity* **7**: 241–253.

Schindelin J, Arganda-Carreras I, Frise E, Kaynig V, Longair M, Pietzsch T, Preibisch S, Rueden C, Saalfeld S, Schmid B et al. 2012. Fiji: an open-source platform for biological-image analysis. *Nature Methods* **9**: 676.

Scholander PF, Hammel H, Bradstreet ED, Hemmingsen E. 1965. Sap pressure in vascular plants. *Science* **148**: 339–346.

Scholz A, Klepsch M, Karimi Z, Jansen S. 2013. How to quantify conduits in wood? *Frontiers in Plant Science* **4**: 56.

Skelton RP, West AG, Dawson TE. 2015. Predicting plant vulnerability to drought in biodiverse regions using functional traits. *Proceedings of the National Academy of Sciences, USA* **112**: 5744–5749.

Smith TB, Wayne RK, Girman DJ, Bruford MW. 1997. A role for ecotones in generating rainforest biodiversity. *Science* **276**: 1855–1857.

Sobrado M. 2009. Leaf tissue water relations and hydraulic properties of sclerophyllous vegetation on white sands of the upper Rio Negro in the Amazon region. *Journal of Tropical Ecology* **25**: 271–280.

Sperry J, Donnelly J, Tyree M. 1988. A method for measuring hydraulic conductivity and embolism in xylem. *Plant, Cell & Environment* **11**: 35–40.

Sperry JS, Hacke UG, Pittermann J. 2006. Size and function in conifer tracheids and angiosperm vessels. *American Journal of Botany* **93**: 1490–1500.

ter Steege H, Sabatier D, Castellanos H, Van Andel T, Duivenvoorden J, De Oliveira AA, Ek R, Lilwah R, Maas P, Mori S. 2000. An analysis of the floristic composition and diversity of Amazonian forests including those of the Guiana Shield. *Journal of Tropical Ecology* **16**: 801–828.

Stocker TF, Qin D, Plattner G-K, Tignor M, Allen SK, Boschung J, Nauels A, Xia Y, Bex B, Midgley B. 2013. *IPCC, 2013: climate change 2013: the physical science basis. Contribution of working group I to the fifth assessment report of the intergovernmental panel on climate change.* Cambridge, UK: Cambridge University Press.

Stropp J, van der Sleen P, Assunção PA, Silva AL, Steege HT. 2011. Tree communities of white-sand and terra-firme forests of the upper Rio Negro. *Acta Amazonica* **41**: 521–544.

Stropp J, van der Sleen P, Quesada CA, ter Steege H. 2014. Herbivory and habitat association of tree seedlings in lowland evergreen rainforest on white-sand and terra-firme in the upper Rio Negro. *Plant Ecology & Diversity* **7**: 255–265.

Targhetta N, Kesselmeier J, Wittmann F. 2015. Effects of the hydroedaphic gradient on tree species composition and aboveground wood biomass of oligotrophic forest ecosystems in the central Amazon basin. *Folia Geobotanica* **50**: 185–205.

Thomas R, Lello J, Medeiros R, Pollard A, Robinson P, Seward A, Smith J, Vafidis J, Vaughan I. 2015. *Data analysis with R statistical software: a guidebook for scientists.* Cardiff, UK: Eco-explore.

Tng DY, Apgaua DM, Ishida YF, Mencuccini M, Lloyd J, Laurance WF, Laurance SG. 2018. Rainforest trees respond to drought by modifying their hydraulic architecture. *Ecology and Evolution* **8**: 12479–12491.

Toledo JJ, Castilho CV, Magnusson WE, Nascimento HE. 2017. Soil controls biomass and dynamics of an Amazonian forest through the shifting of species and traits. *Brazilian Journal of Botany* **40**: 451–461.

Tomasella J, Hodnett MG, Cuartas LA, Nobre AD, Waterloo MJ, Oliveira SM. 2008. The water balance of an Amazonian micro-catchment: the effect of interannual variability of rainfall on hydrological behaviour. *Hydrological Processes: An International Journal* **22**: 2133–2147.

Tuomisto H, Ruokolainen K, Yli-Halla M. 2003. Dispersal, environment, and floristic variation of western Amazonian forests. *Science* **299**: 241–244.

Tyree MT, Vargas G, Engelbrecht BMJ, Kursar TA. 2002. Drought until death do us part: a case study of the desiccation-tolerance of a tropical moist forest seedling-tree, *Licania platypus* (Hemsl.) Fritsch. *Journal of Experimental Botany* **53**: 2239–2247.

Valencia R, Foster RB, Villa G, Condit R, Svenning JC, Hernández C, Romoleroux K, Losos E, Magård E, Balslev H. 2004. Tree species distributions and local habitat variation in the Amazon: large forest plot in eastern Ecuador. *Journal of Ecology* **92**: 214–229.

Venturas MD, MacKinnon ED, Dario HL, Jacobsen AL, Pratt RB, Davis SD. 2016. Chaparral shrub hydraulic traits, size, and life history types relate to species mortality during California's historic drought of 2014. *PLoS ONE* **11**: e0159145.

Webb CO, Donoghue MJ. 2005. Phylomatic: tree assembly for applied phylogenetics. *Molecular Ecology Notes* **5**: 181–183.

Westoby M. 1998. A leaf-height-seed (LHS) plant ecology strategy scheme. *Plant and Soil* **199**: 213–227.

Williamson GB, Wiemann MC. 2010. Measuring wood specific gravity. . . correctly. *American Journal of Botany* **97**: 519–524.

Wittmann F, Householder E, Piedade MTF, de Assis RL, Schöngart J, Parolin P, Junk WJ. 2013. Habitat specifity, endemism and the neotropical distribution of Amazonian white-water floodplain trees. *Ecography* **36**: 690–707.

Wittmann F, Junk WJ. 2016. The Amazon River basin. In: Finlayson CM, Milton GR, Prentice C, Davidson NC, eds. *The wetland book: II: distribution, description and conservation.* Amsterdam, the Netherlands: Springer, 1–20.

Xu X, Medvigy D, Powers JS, Becknell JM, Guan K. 2016. Diversity in plant hydraulic traits explains seasonal and inter-annual variations of vegetation dynamics in seasonally dry tropical forests. *New Phytologist* **212**: 80–95.

Zanne AE, Westoby M, Falster DS, Ackerly DD, Loarie SR, Arnold SE, Coomes DA. 2010. Angiosperm wood structure: global patterns in vessel anatomy and their relation to wood density and potential conductivity. *American Journal of Botany* **97**: 207–215.

Ziegler C, Coste S, Stahl C, Delzon S, Levionnois S, Cazal J, Cochard H, Esquivel-Muelbert A, Goret J-Y, Heuret P et al. 2019. Large hydraulic safety margins protect Neotropical canopy rainforest tree species against hydraulic failure during drought. *Annals of Forest Science* **76**: 115.

Zuleta D, Duque A, Cardenas D, Muller-Landau HC, Davies SJ. 2017. Drought-induced mortality patterns and rapid biomass recovery in a terra firme forest in the Colombian Amazon. *Ecology* **98**: 2538–2546.

Supporting Information

Additional Supporting Information may be found online in the Supporting Information section at the end of the article.

Table S1 Tree species richness, density, DBH and basal area for the four habitats sampled in this study.

Table S2 Summary of the statistical results of the linear fixed-effect models for P_{50} across the four different environments.

Table S3 A summary of the statistical results of the linear mixed-effect models for SM across the four different environments (SM = $\alpha + \beta$ (habitat) + u(species) + ε).

Table S4 Summary of the statistical results of the linear mixed-effect models for SLA, WSG and Nstomata (Trait = $\alpha + \beta$ (soil type * water regime) + u(genus) + ε).

Table S5 Summary of the statistical results of the linear mixed-effect models for the hydraulic traits.

Table S6 Summary of the statistical results of the linear mixed-effect models for the wood anatomy traits.

Table S7 Summary of the statistical results of the linear mixed-effect models for the stable isotope traits.

Table S8 Species mean, minimum and maximum values of the sixteen functional traits. Excel file.

Table S9 Loadings of Axis1 and Axis2 of the PCA-trait (Fig. 6).

Table S10 Summary of the statistical results of the linear mixed-effect models (PCA axis = $\alpha + \beta$ (habitat) + u(genus) + ε) using PCA axis 1 and PCA axis 2 across the four different environments.

Table S11 Pagel's lambda and Blomberg's K for the 16 traits analyzed in this study.

Please note: Wiley Blackwell are not responsible for the content or functionality of any Supporting Information supplied by the authors. Any queries (other than missing material) should be directed to the *New Phytologist* Central Office.

About *New Phytologist*

- *New Phytologist* is an electronic (online-only) journal owned by the New Phytologist Trust, a **not-for-profit organization** dedicated to the promotion of plant science, facilitating projects from symposia to free access for our Tansley reviews and Tansley insights.

- Regular papers, Letters, Research reviews, Rapid reports and both Modelling/Theory and Methods papers are encouraged. We are committed to rapid processing, from online submission through to publication 'as ready' via *Early View* – our average time to decision is <26 days. There are **no page or colour charges** and a PDF version will be provided for each article.

- The journal is available online at Wiley Online Library. Visit **www.newphytologist.com** to search the articles and register for table of contents email alerts.

- If you have any questions, do get in touch with Central Office (np-centraloffice@lancaster.ac.uk) or, if it is more convenient, our USA Office (np-usaoffice@lancaster.ac.uk)

- For submission instructions, subscription and all the latest information visit **www.newphytologist.com**